IRIS AperTO

UNIVERSITÀ DEGLI STUDI DI TORINO

AperTO - Archivio Istituzionale Open Access dell'Università di Torino

Unveiling the interaction between PDT active squaraines with ctDNA: A spectroscopic study

This is a pre print version of the following article:

Original Citation:

Availability:

This version is available http://hdl.handle.net/2318/1790927 since 2021-06-17T12:08:14Z

Published version:

DOI:10.1016/j.saa.2020.119224

Terms of use:

Open Access

Anyone can freely access the full text of works made available as "Open Access". Works made available under a Creative Commons license can be used according to the terms and conditions of said license. Use of all other works requires consent of the right holder (author or publisher) if not exempted from copyright protection by the applicable law.

(Article begins on next page)

14 September 2026

Unveiling the interaction between PDT active squaraines with ctDNA: a spectroscopic study

Cosmin Butnarasu[a], Nadia Barbero[b] Guido Viscardi[b] and Sonja Visentin[a]

[a] *University of Torino, Department of Molecular Biotechnology and Health Science, Via Quarello15, 10135 Torino, Italy*
[b] *University of Torino, Department of Chemistry and NIS Interdepartmental Centre, Via Pietro Giuria 7, 10125 Torino, Italy*

**Corresponding author: Sonja Visentin, sonja.visentin@unito.it*

Keywords: DNA, squaraines, photodynamic therapy (PDT), interaction, groove binders

ABSTRACT

Squaraine dyes are potential photosensitizers in photodynamic therapy (PDT) due to their ability to release reactive oxygen species (ROS) and cause DNA damage. For this reason, the evaluation and determination of the type of interaction between squaraines and DNA is of the utmost importance.

In this study different spectroscopic techniques such as UV-Vis and fluorescence spectroscopies were used to investigate the type of interaction that occurs between two photosensitizers (halogenated squaraines, i.e. Br-C4 and I-C4) and calf thymus DNA (ctDNA). Squaraines were found to bind ctDNA externally following a minor groove binding as they were able to replace Hoechst (a classic groove binder) from the groove of DNA. This binding mode was further supported by iodide quenching studies, ionic strength assay and Florescence Resonance Energy Transfer. Moreover, association (K_A) and dissociation (K_D) constants were obtained and compared with constants of well-known groove binders.

1. Introduction

The living organisms encloses all the genetic information useful for their development and functioning within deoxyribonucleic acid (DNA). As DNA is the key component for organisms well-being, from a pharmaceutical point of view DNA is a central target for most oncologic drugs, as

well as many antiretroviral and antimicrobial agents [1]. Based on the mechanism of interaction with DNA, drugs are distinguished between groove-binders, intercalating, strand-breaking and covalent bonding [2]. Some of these drugs generates harmful reactive oxygen species (ROS) capable to produce DNA damage. Proteins, lipids and nucleic acids are the biological targets of ROS. The alteration induced by ROS usually produce disfunctions of normal activities of the biological targets and that brings eventually to cell death [3,4]. From a clinical point of view the generation of ROS in specific and defined target points in the human body are of utmost importance in photodynamic therapy (PDT). PDT encompasses the topical or systemically administration of a photosensitizer which, after irradiation at an appropriate wavelength, is capable of producing ROS, resulting in damage to target cancer cells in which it is selectively accumulated [3,5]. Recently our group synthesized and studied some series of polymethine dyes demonstrating their ability to release ROS [6,7]. It was shown that in particular two squaraines named Br-C4 and I-C4 are potential photosensitizers for PDT (Figure 1) [6].

Squaraine dyes are the products of dicondensation reactions between electron-rich substrates and squaric acid. In the last two decades great interest was addressed to this class of organic dyes because of their interesting photochemical and photophysical characteristics. Indeed, squaraines display an intense absorption and emission in the red to near infrared region. These photophysical features raised their use in a huge amount of technologies, such as renewable energy [8–11], biological applications [6,12–15] and sensitizers for PDT [5,16,17]. Moreover, different studies have proved that while in dark conditions squaraines are hardly cytotoxic, after irradiation at proper wavelength, they induced a significative phototoxic activity in cancer cells, which was proportional to the squaraine concentration [5,16].

Since small compounds can interact with the double strand of DNA in different ways, it is essential to decipher the mechanism of interaction at molecular level in order to design novel and promising drugs for clinical use. Intercalators and groove binders behave differently with the genetic material: the intercalators insert into the double helix, forming a stronger and more damaging bond with DNA than groove binders. The groove binders, on the other hand, remain on the outside of the double helix, bonding in a less powerful manner; anyway, this still causes DNA damage even if to a lesser extent. These differences on the binding with DNA allow us to discriminate the various bonds through the use of spectrophotometric techniques. Although several papers have been published concerning the photodynamic activity of halogenated squaraines and their damage to DNA [6,16,18], little is known about their mechanism of interaction with DNA. For a better understanding of the mechanism of photobiological activity, in this study, we used several spectrophotometric techniques, like UV-Vis spectroscopy, fluorescence spectroscopy and FRET (Supporting Information), to determine how the squaraines bind to DNA.

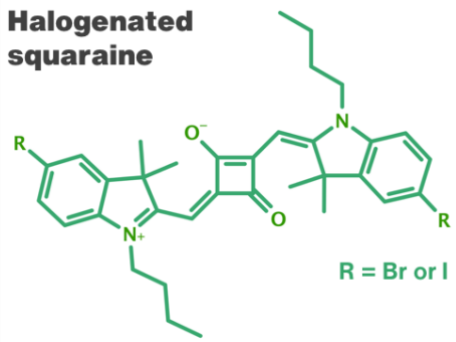

Fig. 1. Molecular structure of the two investigated squaraines.

2. Materials and methods

2.1. Materials

Ethidium bromide (EB), calf thymus DNA (ctDNA) and dimethyl sulfoxide (DMSO) were purchased from Merck and used without further purification. An in-house Millipore system was used to obtain Millipore grade water (resistivity: 18.2 MΩ cm at 25 °C). Squaraines were synthetized as previously reported [6]. TNE buffer was obtained using Picofluor™ protocol. TNE buffer was prepared by dissolving 12.1 g of Tris, 3.7 g of EDTA and 116.9 g of NaCl in 1 L of water. The pH of TNE was adjusted to 7.4 with HCl. All dilutions useful to the various analyses in this study were performed using this particular buffer that provides solutions to the correct ionic strength.

2.2. Sample preparation

ctDNA stock solution was obtained by dissolving it in water under stirring and stored at 0-4 °C in the dark. The concentration of ctDNA stock solution was calculated by measuring the absorbance at 260 nm and using a molar absorption coefficient of 6600 L mol^{-1} cm^{-1}. The purity of DNA solution was checked by calculating the absorbance ratio A_{260}/A_{280}. As the value of the ratio was between 1.8 and 1.9, thus meaning that ctDNA was satisfactorily free from protein, no further purification was required [19,20]. All the working solutions were further prepared by diluting the stock solution in buffer.

Squaraines stock solutions (1 mM) were obtained by dissolving the solid in DMSO and dilutions for the experiments were made in TNE buffer.

2.3. Methods

2.3.1. UV-Vis measurements

A UH5300 Hitachi spectrophotometer and a 1 x 1 cm quartz cuvettes were used to record all the absorption measurements. The UV-Vis spectra of squaraines complexed with ctDNA were measured in the 200–700 nm range. Experiments were carried out by keeping a fixed amount of squaraines, 10 μM, in a total volume of 3 mL and subsequently titrated with increasing concentration (0–77.4 μM) of ctDNA.

2.3.2. Fluorescence measurements

A Horiba Jobin Yvon Fluorolog 3 spectrofluorophotometer and a 1.0 cm quartz cells were used to record all the fluorescence spectra. The fluorescence of ctDNA-EB complex was obtained in the range 585-750 nm upon excitation at 286 nm; slits were set on 5 nm and 3 nm for excitation and emission, respectively. ctDNA and EB concentrations to form the complex were set at 36.7 μM and 10 μM, respectively, in a volume of 3 mL; squaraines concentration was varied from 0–40 μM.

2.3.3. Competitive displacement assays

Hoechst 33258 (HOE) was added to a ctDNA solution in order to study the competitive displacement. The HOE-ctDNA complex containing 1 μM HOE and 10 μM ctDNA was excited at 355 nm. Emission spectra were recorded in the spectral range 375-600 nm. Squaraine was gradually added (0-200 μM) to a constant concentration of HOE-ctDNA complex. The cuvette was filled with TNE buffer to a final volume of 3 mL.

2.3.4. Iodide quenching studies

The iodide quenching tests were accomplished after exciting squaraines and recording the emission spectra in presence of gradually increased amounts of KI, both in absence and presence of ctDNA (50 μM). A total of 3 mL solution comprised 50 μM squaraine, TNE buffer and variable concentration of KI in the range of 0-4 mM. Fluorescence spectra were measured over the spectral range 280-500 nm upon excitation at 260 nm. Fluorescence quenching efficiency both in absence and presence of ctDNA was analyzed using the Stern-Volmer equation.

2.3.5. Role of ionic strength

The effect of ionic strength was investigated by changing the concentration of sodium chloride (NaCl) in the range of 0-90 mM, in a total volume of 3 mL containing 50 μM squaraine, 50 μM ctDNA and TNE buffer. Fluorescence spectra were recorded in the spectral range 280-500 nm and the excitation wavelength was set at 260 nm.

3. Results and discussion

3.1. UV-Vis absorption studies

UV-Vis spectroscopy is one of the simplest and easily reproducible technique used to assess the type of interaction between macromolecules (usually proteins) and small molecules [21]. Through UV-Vis study the structure and the conformation of complexes can be explored. The absorption spectra of squaraines with and without ctDNA were registered and are displayed in Figure 2. Generally, the bound of small molecules to DNA via intercalation, involves the aromatic groups of the chromophore and the DNA base pairs, of whom mechanism of interaction is stacking-based. The resulting maximum of absorption will display bathochromism and a significant hypochromic effect. When intercalation takes place, the probability of electron transition and coupling energy are reduced, thus resulting in a color reduction and a red-shift phenomenon [2,22,23]. On the other hand, if electrostatic interaction occurs, mainly a hyperchromic effect will be observed as a consequence of the changes of the structure and conformation of DNA upon the formation of the complex between the compound and DNA. Generally speaking, when a positively charged compound bind to the negatively charged phosphate groups of DNA backbone, the secondary structure of DNA will shrink and spectroscopically a hyperchromic effect is usually observed [24,25]. Similarly, the groove binding interaction produces an enhancement of the absorption bands, which is proportional to the concentration of DNA[23]. As shown in Figure 2, with the addition of increasing concentration of ctDNA to a SQ dye solution, no bathochromic shifts or hypochromic effects were observed. Actually, upon increasing the concentration of DNA, we recorded an increase of the absorption bands at 596 and 660 nm corresponding to squaraines. These observations suggest that rather than an intercalative mode of interaction between squaraines and ctDNA, an electrostatic or groove binding mode is preferred.

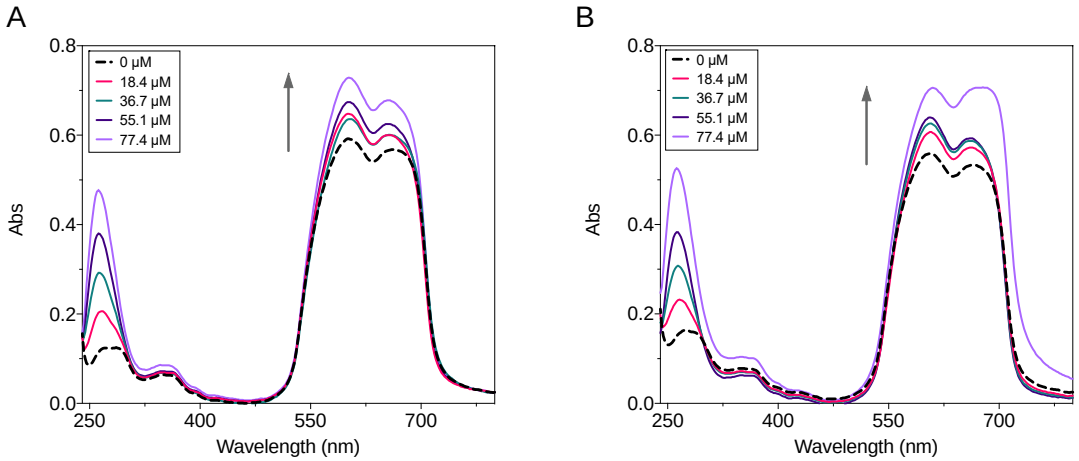

Figure 2. UV-Vis spectra of squaraines-ctDNA interaction. In the spectrum (A) it is represented the interaction between ctDNA and Br-C4 and in the spectrum (B) the interaction between ctDNA and I-C4. The black dashed line represents the absorption spectrum of squaraine alone, while the colored lines represent squaraine absorption spectrum at increasing concentrations of ctDNA.

3.2. Fluorescence quenching mechanism of SQ-ctDNA-EB system

Ethidium bromide (EB) is a planar molecule characterized by a very weak fluorescence in aqueous medium. However, when it intercalates into the base pairs of DNA, it encounters a more hydrophobic environment that forces the loss of any water molecule associated with EB. As water is a very efficient fluorescence quencher the result is a great increase of fluorescence emission [19,26–28]. With this in mind, a complex ctDNA-Ethidium Bromide (EB) was used because the emission spectrum of the ctDNA alone is too low in terms of intensity. The enhanced fluorescence intensity can be turned off by adding a second molecule and the amount of fluorescence quenching can be used to define the binding between the second compound and ctDNA[29]. Figure 3 shows the fluorescence spectra of ctDNA-EB complex upon the increasing concentrations of squaraines (SQ). The fluorescence of ctDNA-EB systems at 605 nm decreased as the amount of squaraines increased. The fluorescence quenching data of the complex SQ-ctDNA-EB were analyzed by three different approaches in order to calculate the equilibrium association (K_A) and dissociation (K_D) constants. For the SQ-ctDNA-EB system, two possible reasons describe the reduction of the ctDNA-EB emission upon addition of SQ. The first reason consists in replacement of the intercalated EB from the double strand which decreases the concentration of EB binding to ctDNA. The second reason is the turn off the fluorescence of ctDNA-EB complex by bond of SQ [1]. The absorption measurements suggest that the binding mechanism between SQ and ctDNA was not relying on intercalation but more likely on electrostatic or groove binding modes. Moreover, based on the values of binding constant reported in Table 1, we can state that the replacement of EB from ctDNA was not possible as the binding constant of EB-DNA is 5.16×10^5 mol L^{-1} as reported by Ramana et al. [19,26], while for the SQ-ctDNA-EB system, binding constant are on average 5 fold lower. To confirm this hypothesis further investigation were conducted.

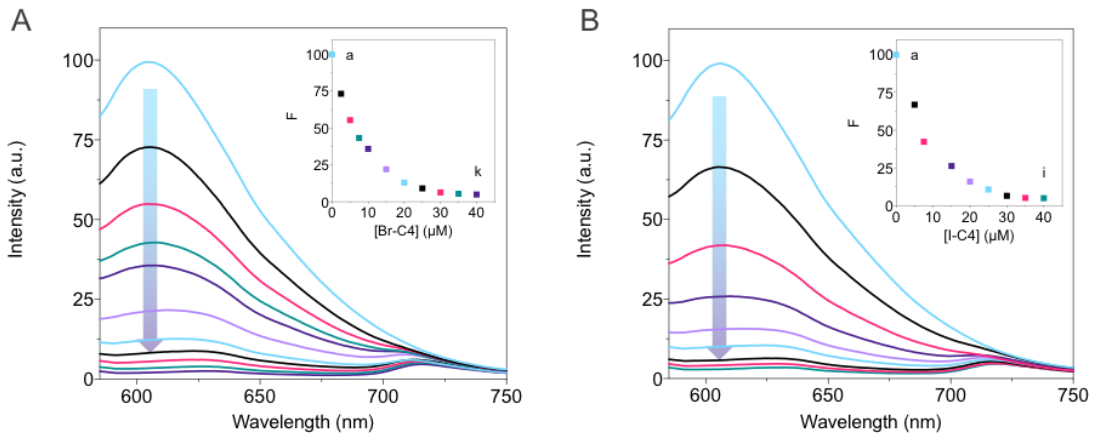

Figure 3. Fluorescence spectra of SQ-ctDNA-EB. (A) Interaction between ctDNA-EB and Br-C4 and (B) interaction of ct-DNA-EB and I-C4. The most intensive light blue lines represent emission spectra of ctDNA-EB complex; all the other colored lines are the emission spectra of interactions between ctDNA-EB and squaraines. $[Br\text{-}C4]_{a\text{-}k}$ = 0, 2.5, 5, 7.5, 10, 15, 20, 25, 30, 35, 40 μM; $[I\text{-}C4]_{a\text{-}i}$ = 0, 5, 7,5, 15, 20, 25, 30, 35, 40 μM. The insets represent the variation of the maximum of fluorescence upon increasing the concentration of squaraine.

3.2.1. Stern-Volmer equation

The fluorescence quenching data of SQ-ctDNA-EB complex were analyzed according to Stern–Volmer equation (Eq.1)

$$\frac{F_0}{F} = 1 + K_{SV}[Q] \qquad (Eq.\,1)$$

where F_0 is the fluorescence intensity of ctDNA-EB alone and F is the fluorescence intensity of the complex in presence of increased concentration of squaraine, K_{SV} is the Stern–Volmer quenching constant and [Q] is the squaraine concentration. Quenching data are presented as plots of F_0/F versus [Q], yielding an intercept of one on the y-axis and a slope equal to K_{SV}. The fluorescence quenching of ctDNA-EB upon binding to SQ shows positive deviation from the Stern-Volmer equation. This tendency is often observed when the extent of quenching is large. In such events, usually only the linear part of the plot is fitted to Stern-Volmer equation (insets on Figure 4A and 4B), in order to gain information about the SQ-ctDNA-EB interaction constant [30].

3.2.2. Non-linear least squares

Data were fitted also according to a non-linear fit method, based on Equation 2:

$$y = \frac{(B_{max} \cdot [Q])}{(K_D + [Q])} \qquad (Eq.\,2)$$

where, *y* is the explicit binding obtained by measuring fluorescence intensity, Bmax is the maximum extent of the complex SQ-ctDNA-EB created at saturation and K_D is the equilibrium

dissociation constant. Since in a biomolecular reaction at equilibrium the K_D and K_A are mutually correlated, we calculated K_A as the reciprocal of K_D. The binding curves are displayed in Figure 4 (C and D); the percentage of bound ctDNA, that is, the ordinate axis, calculated from the emission maximum intensities, is plotted against the squaraines concentration. The K_A and K_D values are reported in Table 1.

3.2.3. Lineweaver-Burk

Another frequently used method to linearize data is the Lineweaver–Burk equation based on Equation 3:

$$\frac{1}{(F_0 - F)} = \frac{1}{F_0} + \frac{K_D}{F_0 \cdot [Q]} \qquad (Eq. 3)$$

In Figure 4 the reciprocals of F_0–F are plotted against reciprocals of [Q]. K_D/F_0 ratio is the slope of the line while F_0 is the reverse of the intercept. The equilibrium dissociation (K_D) and association (K_A) constants are thus easily calculated and are reported in Table 1.

As reported in Table 1, we can observe that constants obtained with different analysis methods perfectly agree to each other. Association constants are in the order of 10^5 M^{-1} which is appreciably lower than that of the intercalation binding mode. The K_A of classic intercalators such as ruthenium complexes are reported to be around 10^6 M^{-1} [31,32], while even higher values on the order of 10^7 M^{-1} were reported for anthracycline as daunorubicin [33,34]. The value of the obtained binding constants is an indirect confirmation of the mode of interaction of squaraine with DNA.

Table 1. Association (K_A) and Dissociation (K_D) constants at 25 °C calculated with different mathematical models.

	Stern-Volmer	**Non-Linear Fit**		**Lineweaver-Burk**	
	K_{SV} ($\cdot 10^5$ M^{-1})	K_D ($\cdot 10^{-6}$ M)	K_A ($\cdot 10^5$ M^{-1})	K_D ($\cdot 10^{-6}$ M)	K_A ($\cdot 10^5$ M^{-1})
Br-C4	2.10	8.40	1.19	8.92	1.12
I-C4	2.09	7.39	1.35	8.38	1.19

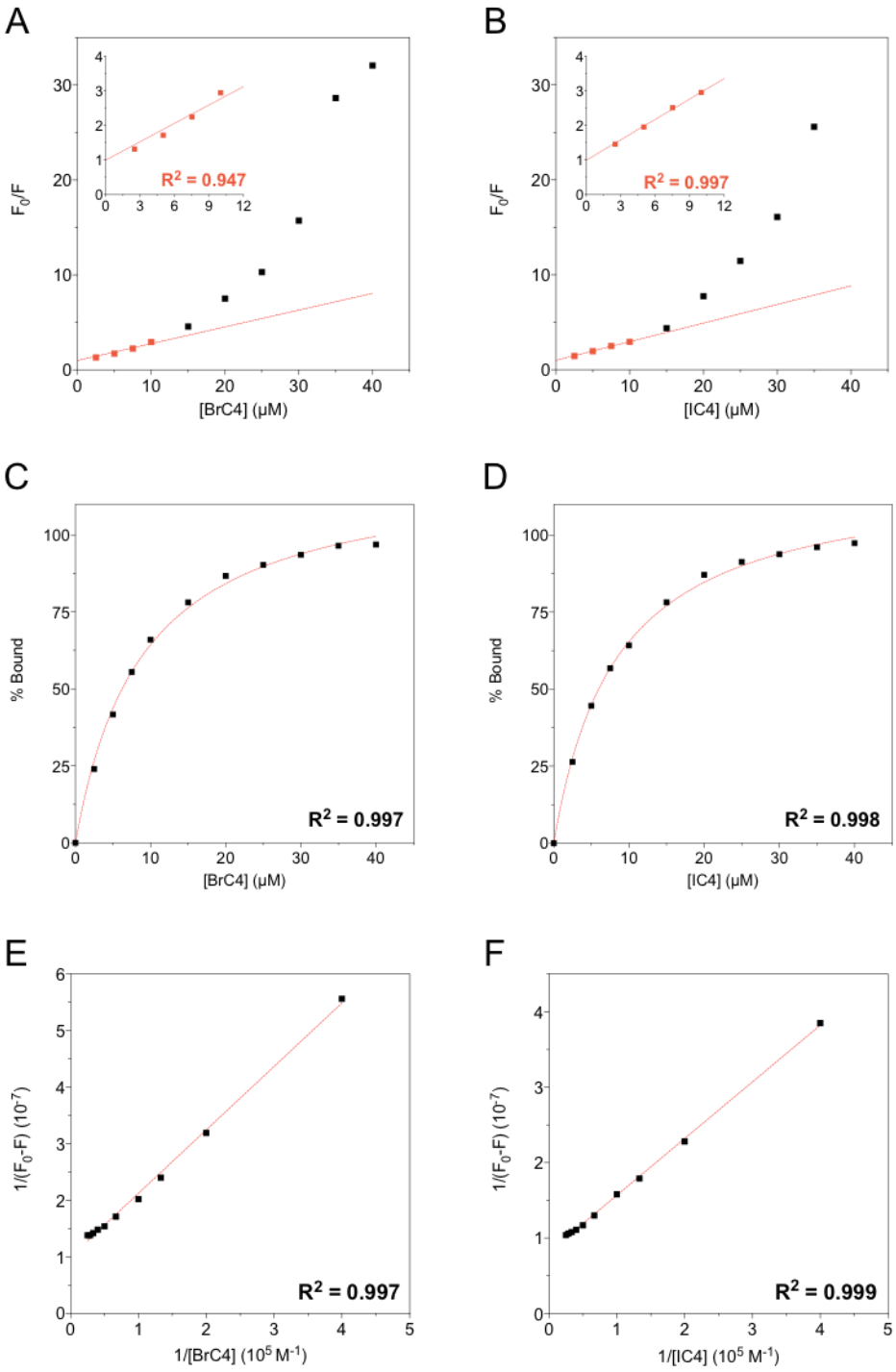

Figure 4. Data analysis of fluorescence quenching. In the spectra (A) and (B) are represented the Stern-Volmer analysis of BrC4-ctDNA-Eb and IC4-ctDNA-EB interactions, respectively. The insets on (A) and (B) reports the linear tract of the Stern-Volmer plot. In the spectra (C) and (D) are represented the non-linear least squares analysis of the same interactions. At last, in the spectra (E) and (F) are represented the Lineweaver-Burk analysis of the interactions.

3.3 Competitive Displacement Assay

To better understand how squaraines bind DNA, we carried out competitive binding experiments. In this experiment, Hoechst 33258, a commonly used minor groove binder of DNA with high specificity for AT-rich sequences, was employed to study the competitive replacement by groove binders [1,20,21]. Hoechst 33258 has a very weak fluorescence intensity in aqueous solutions however, on binding with DNA, it shows an increase in the fluorescence intensity characterized by a strong band at 458 nm [26,35]. Molecules that bind DNA via groove binding mode can replace Hoechst 33258 from the minor groove of DNA that resulting in quenching of fluorescence of the band at 458 nm, which corresponds to the DNA-Hoechst system. As shown in Figure 5, upon addition of gradually increased squaraine concentration, the fluorescence intensity of Hoechst-ctDNA complex was found to diminish. This spectroscopic response can be explained as squaraines gradually replaced the groove bounded dye from ctDNA. This result suggests that rather than intercalation, there is a high probability that the binding of squaraine to ctDNA involves the minor groove sites, as indeed proved by squaraine ability to displace Hochest. This hypothesis was further evaluated by performing iodide quenching experiment.

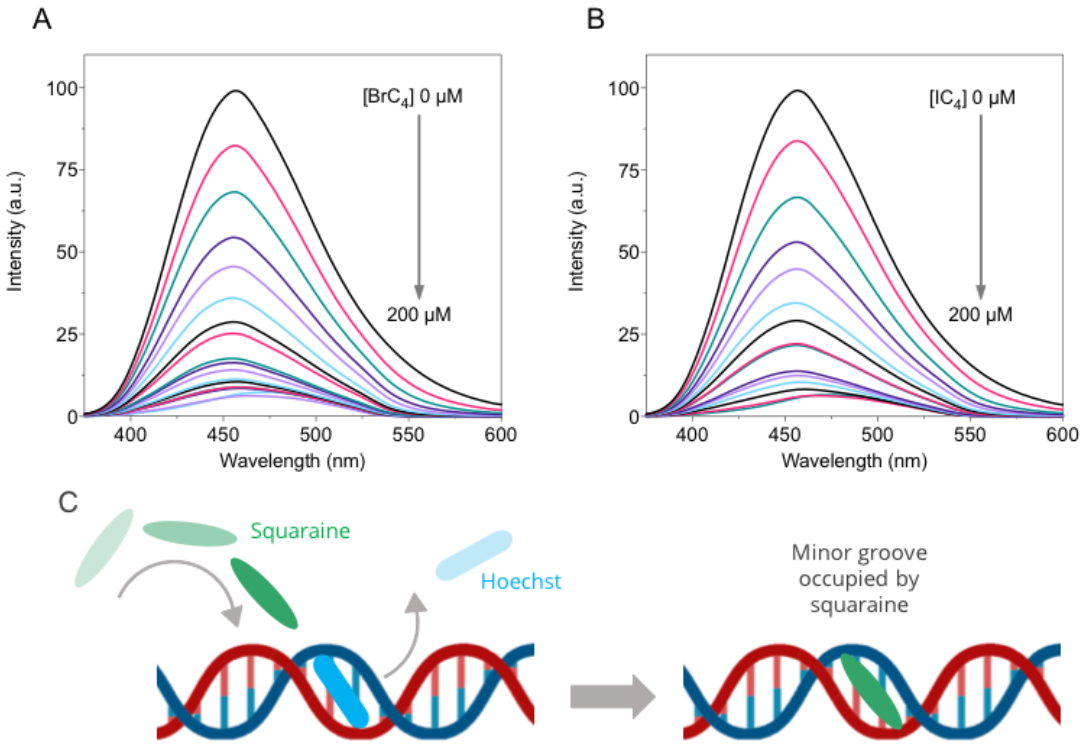

Figure 5. Fluorescent intensity of Hoechst-ctDNA in presence of increasing concentrations of Br-C4 (A) and I-C4 (B). $[Br\text{-}C4]_{a\text{-}r}$ = 0, 5, 10, 15, 20, 25, 30, 35, 40, 45, 50, 60, 70, 80, 90, 100, 150,

200 μM; $[I\text{-}C4]_{a\text{-}o}$ = 0, 5, 10, 15, 20, 25, 30, 35, 40, 50, 60, 80, 100, 150, 200 μM. Schematic representation of the displacement of Hoechst by squaraine on the minor groove (C).

3.4 Iodide Quenching Study

Iodide ion quenching experiments are useful on understanding if the location of the bonded molecules is placed either outside or inside of DNA helix. Iodide ions are known to turn off the fluorescence of small compounds in aqueous environments. When DNA is present, the negative charges on the phosphate groups repeal the iodide ions. If a small compound intercalates the double strand of DNA, then it will be well protected, as the contact with negatively charged molecules (such as iodide ions) toward such compound will be restricted because of electrostatic repulsion. Though, molecules that bind DNA preferably by groove binding or electrostatic mechanism, meaning that these molecules are exposed to the surrounding environment, will be susceptible to the attack of quenchers present in the free medium even when DNA is present [20,21]. The level of accessibility of small compounds to negatively charged quenchers in the environment and in presence of ctDNA is described by K_{SV} that can be calculated using Stern-Volmer equation (see Eq. 1 and Figure 6). Reduction in the magnitude of Ksv in presence of DNA is achieved with intercalation, though for groove binders or electrostatic interaction, it remains mostly unaffected. In Figure 6, is reported that KI could efficiently quench the emission of squaraines. However, the presence of ctDNA, produce a slight increase of the Ksv value. The calculated K_{SV} values in the absence and presence of ctDNA for Br-C4 by KI was found to be 38 and 70 M respectively, while for I-C4 the K_{SV} values are 20 and 34 mol L^{-1} respectively. The magnitude of quenching of squaraines that we observe in the presence and in the absence of ctDNA is almost unchanged and therefore, there is a higher probability that the interaction of squaraines with DNA take place outside the DNA helix. Taking together the competitive displacement assay and the iodide quenching study, we can state with more confidence that the binding of squaraines to ctDNA is mainly guided by groove binding interaction.

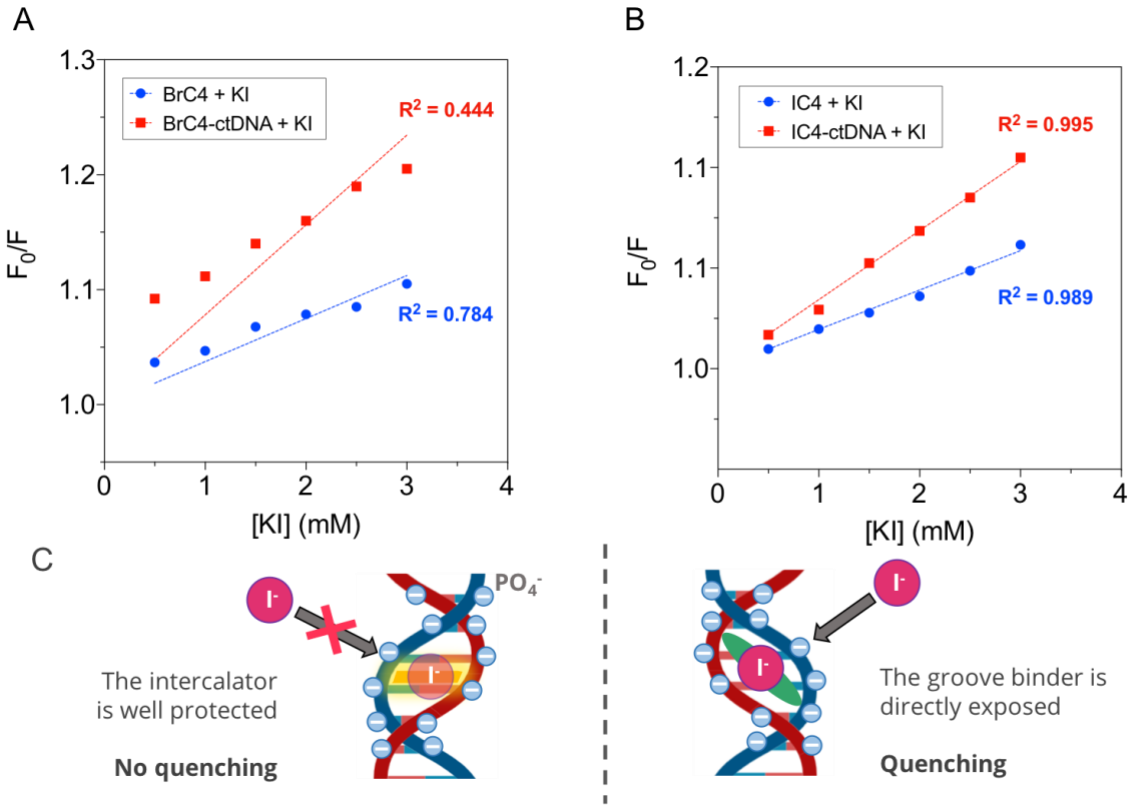

Figure 6. Stern-Volmer plots for fluorescence quenching of Br-C4 (A) and I-C4 (B) by KI in the absence and presence of ctDNA (50 µM). Concentrations of KI was varied from 0.5 to 3 mM. Schematic representation of the mechanism of quenching of fluorescence of the groove binders by action of iodide (C). While intercalators are well protected by being inserted between nucleotides, groove binders are directly exposed to the surrounding environment.

3.5 Effect of Ionic Strength

Another methodology used to discriminate the binding between small compounds and ctDNA is the investigation of ionic strength on the system. Normally, strong electrolyte as sodium chloride (NaCl) is used for this assay. After solubilization, Na^+ partially neutralizes the anionic helix of DNA so reducing the electrostatic repulsion between DNA strands. Small molecules that intercalate into the adjacent base pairs of DNA will be shielded from the surrounding solvent and so the emission intensity will be almost unvaried with the increasing of the concentration of NaCl [36]. In case of surface binding molecules, particularly for electrostatic-dependent binding, the bound with DNA takes place outside the groove; in this case NaCl will reduce the interaction which will be translated in the reduction of emission intensity. Nonetheless, for groove binding molecules, with the increasing of the concentration of NaCl a proportional decrease of fluorescence intensity is usually observed. The increased ionic strength shrinks and deepens the DNA grooves. The

induced structure modification of the helix cause the release of the grove bonded molecule and that translates in the decrease of fluorescence intensity [11,37]. So, the effect of NaCl on the fluorescence of ctDNA-squaraine were studied. The experimental results indicate that the fluorescence intensities of ctDNA-squaraine was decreased with increasing of NaCl concentration (Figure 7). These results can further confirm that the interaction between ctDNA and squaraines is groove binding related.

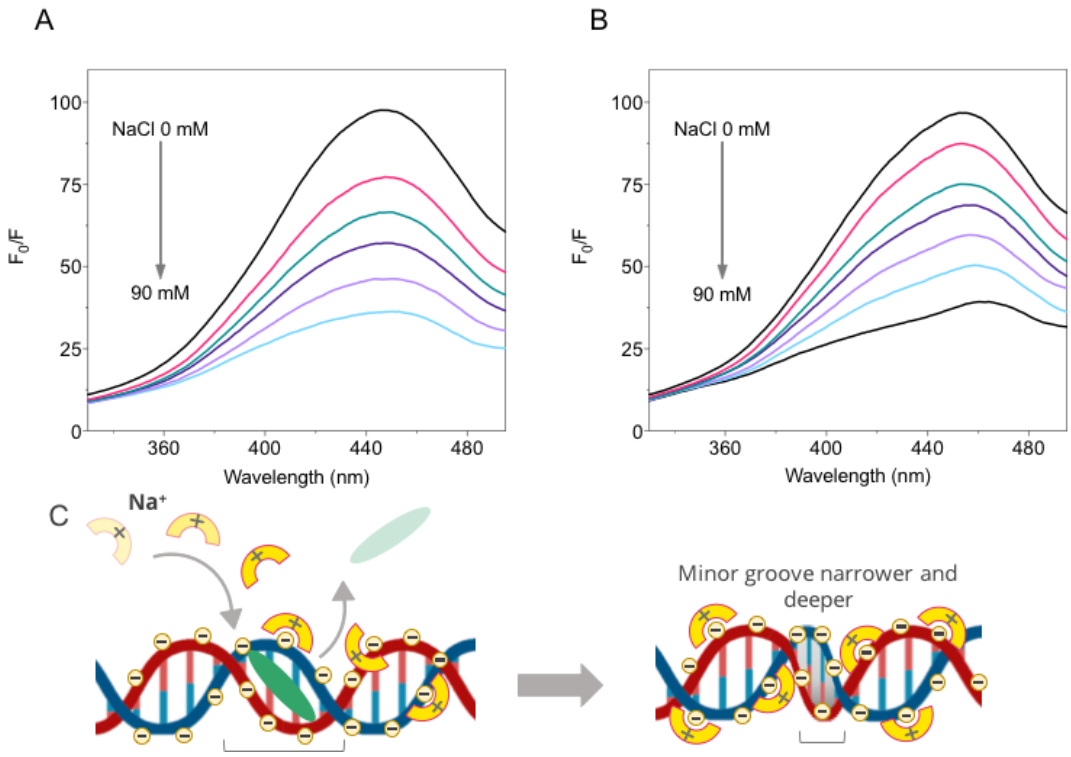

Figure 7. Effects of ionic strength on the fluorescence intensity of Br-C4-ctDNA (A) and I-C4-ctDNA (B). Schematic representation of the ionic strength on the structure of DNA and the implication of squaraine accommodation into the minor groove (C).

4. Conclusions

In this study the interaction between ctDNA and Br- and I-C4 squaraines has been studied through different spectroscopic techniques. Based on the data collected by absorption and emission spectroscopies, displacement assay, iodide quenching study, ionic strength effect and FRET (Supporting Information) data, we can state that the binding mode of squaraine with DNA was disclosed as minor groove binding. The squaraines have a K_A order of 10^5 M^{-1}. Considering that the order of magnitude of association constant of groove binders is usually known to be around 10^3 M^{-1} [38,39], we conclude that Br- and I-C4 have quite a high affinity for ctDNA. This work is

expected to provide deeper insight into understanding the mechanism of interaction of squaraines with DNA and the knowledge gained from this study could be used for the development of potential probes for DNA as well as more selective and efficient photodynamic therapy agents.

Declaration of competing interests

The authors declare that they have no known competing financial interests or personal relationships that could have appeared to influence the work reported in this paper.

Acknowledgments

The authors acknowledge the financial support from the University of Torino (Ricerca Locale ex-60%, Bando 2019) and from the Fondazione Cassa di Risparmio (CRT) di Torino, Italy.

References

[1] M.M.V. Ramana, R. Betkar, A. Nimkar, P. Ranade, B. Mundhe, S. Pardeshi, In vitro DNA binding studies of antiretroviral drug nelfinavir using ethidium bromide as fluorescence probe, J. Photochem. Photobiol. B Biol. 151 (2015) 194–200. https://doi.org/10.1016/j.jphotobiol.2015.08.012.

[2] K. Nakamoto, M. Tsuboi, G.D. Strahan, Drug–DNA Interactions: Structures and Spectra, Wiley, 2008.

[3] A.M. Rkein, D.M. Ozog, Photodynamic Therapy, Dermatol. Clin. 32 (2014) 415–425. https://doi.org/10.1016/j.det.2014.03.009.

[4] H. Abrahamse, M.R. Hamblin, New photosensitizers for photodynamic therapy, Biochem. J. 473 (2016) 347–364. https://doi.org/10.1042/BJ20150942.

[5] R.R. Avirah, D.T. Jayaram, N. Adarsh, D. Ramaiah, Squaraine dyes in PDT: from basic design to in vivo demonstration, Org. Biomol. Chem. 10 (2012) 911–920. https://doi.org/10.1039/C1OB06588B.

[6] L. Serpe, S. Ellena, N. Barbero, F. Foglietta, F. Prandini, M.P. Gallo, R. Levi, C. Barolo, R. Canaparo, S. Visentin, Squaraines bearing halogenated moieties as anticancer photosensitizers: Synthesis, characterization and biological evaluation, Eur. J. Med. Chem. 113 (2016) 187–197. https://doi.org/10.1016/j.ejmech.2016.02.035.

[7] B. Ciubini, S. Visentin, L. Serpe, R. Canaparo, A. Fin, N. Barbero, Design and synthesis of symmetrical pentamethine cyanine dyes as NIR photosensitizers for PDT, Dye.

Pigment. 160 (2019) 806–813. https://doi.org/10.1016/j.dyepig.2018.09.009.
[8] J. Park, N. Barbero, J. Yoon, E. Dell'Orto, S. Galliano, R. Borrelli, J.H. Yum, D. Di Censo, M. Grätzel, M.K. Nazeeruddin, C. Barolo, G. Viscardi, Panchromatic symmetrical squaraines: A step forward in the molecular engineering of low cost blue-greenish sensitizers for dye-sensitized solar cells, Phys. Chem. Chem. Phys. 16 (2014) 24173–24177. https://doi.org/10.1039/c4cp04345f.
[9] J. Park, C. Barolo, F. Sauvage, N. Barbero, C. Benzi, P. Quagliotto, S. Coluccia, D. Di Censo, M. Grätzel, M.K. Nazeeruddin, G. Viscardi, Symmetric vs. asymmetric squaraines as photosensitisers in mesoscopic injection solar cells: A structure-property relationship study, Chem. Commun. 48 (2012) 2782–2784. https://doi.org/10.1039/c2cc17187b.
[10] D. Saccone, S. Galliano, N. Barbero, P. Quagliotto, G. Viscardi, C. Barolo, Polymethine Dyes in Hybrid Photovoltaics: Structure–Properties Relationships, European J. Org. Chem. 2016 (2016) 2244–2259. https://doi.org/10.1002/ejoc.201501598.
[11] S. Kashanian, S. Javanmardi, A. Chitsazan, M. Paknejad, K. Omidfar, Fluorometric study of fluoxetine DNA binding, J. Photochem. Photobiol. B Biol. 113 (2012) 1–6. https://doi.org/10.1016/j.jphotobiol.2012.04.002.
[12] N. Barbero, C. Butnarasu, S. Visentin, C. Barolo, Squaraine Dyes: Interaction with Bovine Serum Albumin to Investigate Supramolecular Adducts with Aggregation-Induced Emission (AIE) Properties, Chem. - An Asian J. 14 (2019) 896–903. https://doi.org/10.1002/asia.201900055.
[13] M. Shimi, V. Sankar, M.K.A. Rahim, P.R. Nitha, S. Das, K. V. Radhakrishnan, K.G. Raghu, Novel glycoconjugated squaraine dyes for selective optical imaging of cancer cells, Chem. Commun. 53 (2017) 5433–5436. https://doi.org/10.1039/c6cc10282d.
[14] G.M. Paternò, L. Moretti, A.J. Barker, C. D'Andrea, A. Luzio, N. Barbero, S. Galliano, C. Barolo, G. Lanzani, F. Scotognella, Correction: Near-infrared emitting single squaraine dye aggregates with large Stokes shifts, J. Mater. Chem. C. 5 (2017) 11144. https://doi.org/10.1039/C7TC90165H.
[15] G. Alberto, N. Barbero, C. Divieto, E. Rebba, M.P. Sassi, G. Viscardi, G. Martra, Solid silica nanoparticles as carriers of fluorescent squaraine dyes in aqueous media: Toward a molecular engineering approach, Colloids Surfaces A Physicochem. Eng. Asp. 568 (2019) 123–130. https://doi.org/10.1016/j.colsurfa.2019.01.052.
[16] D. Ramaiah, I. Eckert, K.T. Arun, L. Weidenfeller, B. Epe, Squaraine Dyes for Photodynamic Therapy: Study of Their Cytotoxicity and Genotoxicity in Bacteria and Mammalian Cells, Photochem. Photobiol. 76 (2002) 672–677. https://doi.org/10.1562/0031-8655(2002)0760672SDFPTS2.0.CO2.
[17] I. Miletto, A. Fraccarollo, N. Barbero, C. Barolo, M. Cossi, L. Marchese, E. Gianotti, Mesoporous silica nanoparticles incorporating squaraine-based photosensitizers: a

combined experimental and computational approach, Dalt. Trans. 47 (2018) 3038–3046. https://doi.org/10.1039/C7DT03735J.

[18] D. Ramaiah, I. Eckert, K.T. Arun, L. Weidenfeller, B. Epe, Squaraine Dyes for Photodynamic Therapy: Mechanism of Cytotoxicity and DNA Damage Induced by Halogenated Squaraine Dyes Plus Light (>600 nm), Photochem. Photobiol. 79 (2004) 99. https://doi.org/10.1562/0031-8655(2004)79<99:sdfptm>2.0.co;2.

[19] Y. Cui, E. Hao, G. Hui, W. Guo, F. Cui, Investigations on the interactions of diclofenac sodium with HSA and ctDNA using molecular modeling and multispectroscopic methods, Spectrochim. Acta Part A Mol. Biomol. Spectrosc. 110 (2013) 92–99. https://doi.org/10.1016/J.SAA.2013.01.093.

[20] S.U. Rehman, T. Sarwar, H.M. Ishqi, M.A. Husain, Z. Hasan, M. Tabish, Deciphering the interactions between chlorambucil and calf thymus DNA: A multi-spectroscopic and molecular docking study, Arch. Biochem. Biophys. 566 (2015) 7–14. https://doi.org/10.1016/j.abb.2014.12.013.

[21] M.A. Husain, T. Sarwar, S.U. Rehman, H.M. Ishqi, M. Tabish, Ibuprofen causes photocleavage through ROS generation and intercalates with DNA: a combined biophysical and molecular docking approach, Phys. Chem. Chem. Phys. 17 (2015) 13837–50. https://doi.org/10.1039/c5cp00272a.

[22] R. Arif, P.S. Nayab, Akrema, M. Abid, U. Yadava, Rahisuddin, Investigation of DNA binding and molecular docking propensity of phthalimide derivatives: in vitro antibacterial and antioxidant assay, J. Anal. Sci. Technol. 10 (2019) 1–9. https://doi.org/10.1186/s40543-019-0177-1.

[23] Y. Yang, J.Y. Bian, Y.H. Li, H.C. Guan, Y.R. Tang, Y.L. Chen, S.M. Yue, Construction of six complexes from 2-(2-pyridyl)benzothiazole and polycarboxylic acids: Synthesis, crystal structures and DNA-binding properties, J. Mol. Struct. (2020). https://doi.org/10.1016/j.molstruc.2019.127219.

[24] F. Arjmand, A. Jamsheera, DNA binding studies of new valine derived chiral complexes of tin(IV) and zirconium(IV), Spectrochim. Acta - Part A Mol. Biomol. Spectrosc. (2011). https://doi.org/10.1016/j.saa.2010.06.009.

[25] M. Sirajuddin, S. Ali, A. Badshah, Drug–DNA interactions and their study by UV–Visible, fluorescence spectroscopies and cyclic voltametry, J. Photochem. Photobiol. B Biol. 124 (2013) 1–19. https://doi.org/10.1016/J.JPHOTOBIOL.2013.03.013.

[26] M.M.V. Ramana, R. Betkar, A. Nimkar, P. Ranade, B. Mundhe, S. Pardeshi, Synthesis of a novel 4H-pyran analog as minor groove binder to DNA using ethidium bromide as fluorescence probe, Spectrochim. Acta - Part A Mol. Biomol. Spectrosc. 152 (2016) 165–171. https://doi.org/10.1016/j.saa.2015.07.037.

[27] R. Gaur, M. Usman, A combined experimental and theoretical investigation of ruthenium(II)-hydrazone complex with DNA: Spectroscopic, nuclease activity,

topoisomerase inhibition and molecular docking, Spectrochim. Acta Part A Mol. Biomol. Spectrosc. 209 (2019) 100–108. https://doi.org/10.1016/J.SAA.2018.10.035.
[28] J. Olmsted, D.R. Kearns, Mechanism of Ethidium Bromide Fluorescence Enhancement on Binding to Nucleic Acids, Biochemistry. 16 (1977) 3647–3654.
[29] M.M. Aleksić, V. Kapetanović, An overview of the optical and electrochemical methods for detection of DNA - Drug interactions, Acta Chim. Slov. 61 (2014) 555–573.
[30] M. Airoldi, G. Barone, G. Gennaro, A.M. Giuliani, M. Giustini, Interaction of doxorubicin with polynucleotides. a spectroscopic study, Biochemistry. 53 (2014) 2197–2207. https://doi.org/10.1021/bi401687v.
[31] S. Mardanya, S. Karmakar, D. Maity, S. Baitalik, Ruthenium(II) and osmium(II) mixed chelates based on pyrenyl-pyridylimidazole and 2,2′-bipyridine ligands as efficient DNA intercalators and anion sensors, Inorg. Chem. 54 (2015) 513–526. https://doi.org/10.1021/ic502271k.
[32] E. Wachter, D. Moyá, S. Parkin, E.C. Glazer, Ruthenium Complex “Light Switches” that are Selective for Different G-Quadruplex Structures, Chem. - A Eur. J. 22 (2016) 550–559. https://doi.org/10.1002/chem.201503203.
[33] Y. Lu, J. Lv, G. Zhang, G. Wang, Q. Liu, Interaction of an anthracycline disaccharide with ctDNA: Investigation by spectroscopic technique and modeling studies, Spectrochim. Acta - Part A Mol. Biomol. Spectrosc. 75 (2010) 1511–1515. https://doi.org/10.1016/j.saa.2010.02.008.
[34] A.A. Almaqwashi, T. Paramanathan, I. Rouzina, M.C. Williams, Mechanisms of small molecule-DNA interactions probed by single-molecule force spectroscopy, Nucleic Acids Res. 44 (2016) 3971–3988. https://doi.org/10.1093/nar/gkw237.
[35] J.H. Shi, J. Chen, J. Wang, Y.Y. Zhu, Binding interaction between sorafenib and calf thymus DNA: Spectroscopic methodology, viscosity measurement and molecular docking, Spectrochim. Acta - Part A Mol. Biomol. Spectrosc. (2015). https://doi.org/10.1016/j.saa.2014.09.056.
[36] N. Akbay, Z. Seferoğlu, E. Gök, Fluorescence interaction and determination of calf thymus DNA with two ethidium derivatives, J. Fluoresc. 19 (2009) 1045–1051. https://doi.org/10.1007/s10895-009-0504-9.
[37] S. Bi, T. Zhao, Y. Wang, H. Zhou, B. Pang, T. Gu, Binding studies of terbutaline sulfate to calf thymus DNA using multispectroscopic and molecular docking techniques, Spectrochim. Acta - Part A Mol. Biomol. Spectrosc. (2015). https://doi.org/10.1016/j.saa.2015.06.042.
[38] D. Sahoo, P. Bhattacharya, S. Chakravorti, Quest for mode of binding of 2-(4-(dimethylamino)styryl)-1-methylpyridinium iodide with calf thymus DNA, J. Phys. Chem. B. 114 (2010) 2044–2050. https://doi.org/10.1021/jp910766q.
[39] B. Jana, S. Senapati, D. Ghosh, D. Bose, N. Chattopadhyay, Spectroscopic exploration

of mode of binding of ctDNA with 3-hydroxyflavone: A contrast to the mode of binding with flavonoids having additional hydroxyl groups, J. Phys. Chem. B. 116 (2012) 639–645. https://doi.org/10.1021/jp2094824.